Supplemental Material: de Jong, Afjei et al.

Figure S1. *In vivo* dual fiber photometry of DA terminals across different NAc subregions during aversive conditioning, Related to Figure 1.
(A) Freezing in response to the tone before conditioning (first shock trial) and after conditioning (last shock trial; first: 14.40 ± 9.27%, n=5; last: 80.60 ± 10.78%, n = 5; ** $p < 0.01$, paired Student's t-test; data represent means ± SEM).
(B, C) Representative examples of raw 470 nm and fitted 405 nm signals from DA terminals simultaneously recorded in the NAcLat (B) and vNAcMed (C). Note that the fitted 405 nm signal is subtracted from the 470 nm signal to obtain the movement- and bleaching-corrected signal (as shown in **Figure 1 and Supplementary Movie 1**).
(D) Although the area under the curve during shock exposure was not significantly different in ventral NAcMed DA terminals (**Figure 1I**, inset), we observed a significant phasic increase in fluorescence activity immediately after shock onset compared to omission trials (Shock: 1.38 ± 0.20; Omission: 0.98 ± 0.13, n = 11 mice; * $p < 0.05$, paired Student's t-test). This is consistent with an aversion prediction error as shock occurrence was uncertain (67%-foot shock probability; data represent means ± SEM).
(E) Coronal brain section showing DA terminals expressing GCaMP6m (green), TH-immunostaining (red) and location of fiber implants in the NAcLat, ventral NAcMed, dorsal NAcMed and NAcCore as well as a sample fluorescence image showing fiber placement from a recording that lacked an excitatory or inhibitory response to foot shock (ac: anterior commissure; scale bars: 200 μm). N = 2 mice lacked an excitatory or inhibitory response to foot shock. These animals had recording-sites that were outside the ventral striatal target region.

Figure S2. Average Z-score responses for individual, well-trained animals during a reward conditioning trial, Related to Figure 2.
Simultaneous recordings from individual animals in the NAcLat (A) and ventral NAcMed (B) that were used for the data shown in Figure 2.

Figure S3. Monosynaptic rabies virus tracing of vNAcMed- and NAcLat-projecting DA neurons using automated segmentation arithmetic, Related to Figure 3.
(A) Fluorescence images showing GFP-positive cells in the ventral striatum (left) and automated segmentation (right, positive pixels in white; scale bar: 50 μm).
(B) Segmented pixels were semi-automatically assigned to defined brain structures, e.g., LH (top), VTA (middle) and DR (bottom). Designated pixels are in red while other GFP-positive pixels are in white (scale bar: 500 μm).
(C) Graph showing high correlation between manually scoring of input neurons by an independent observer and the automated segmentation procedure.
(D) vNAcMed-projecting starter cells were located in the ventromedial VTA (mVTA, green, left panel, IPN: interpeduncular nucleus). Starter cell populations in the VTA were defined as GFP- and TVA-mCherry-positive cells. Bar graph shows co-localization analysis of starter cells with TH (100% TH-immunopositive), non-starter TVA-mCherry-positive cells (100% TH-immunopositive) and secondary (TVA-mCherry-negative) cells (6.52% TH-immunopositive). The right panel shows a sample confocal image of vNAcMed-projecting starter cells (green: RV-ΔG-GFP, red: TVA-mCherry, blue: TH; scale bar: 10 μm).
(E) Same as in (D) but for NAcLat-projecting starter cells, which were mainly located in the

lateral VTA (lVTA). Starter cells and TVA-mCherry-positive cells were 100% TH-immunopositive, while secondary cells were 13.5% TH-immunopositive.

Abbreviations used in Figure 3D: OFC: orbital frontal cortex, mPFC: medial prefrontal cortex, DMS: dorsomedial striatum, DLS: dorsolateral striatum, VP: ventral pallidum, BNST: bed nucleus of the stria terminalis, GP: globus pallidus, PO: preoptic area, LH: lateral hypothalamus, PVN: periventricular nucleus, CeA: central amygdala, LHb: lateral habenula, MHb: medial habenula, STh: subthalamic nucleus, DR: dorsal raphe nucleus, LDT: laterodorsal tegmentum, LPB: lateral parabrachial nucleus.

Figure S4. Serial reconstructions of viral injection sites and anatomical locations of optical fiber implants, Related to Figures 4 and 5.
(A) Coronal brain sections showing ChR2-eYFP (green) expression in the lateral hypothalamus (LH). Top: Left panels show representative examples of ChR2-eYFP injection sites across the rostro-caudal extent of the LH. Right panels show schematics of the corresponding brain regions in which ChR2-eYFP was detected. Each color represents the expression profile from a single mouse that was used for the experiments shown in **Figures 4A-4F**. Blue color code represents example images shown in the left panels (scale bar: 500 μm, f: fornix, LPO: lateral preoptic area). Bottom: Schematics showing anatomical location of fiber implants in the midbrain.
(B, C) Same as in (A) but for NpHR3.0-eYFP expression in the LH of individual mice used for the experiments shown in **Figures 4G-4M** (B) and for GCaMP6m expression in the LH of individual mice used for the experiments shown in **Figures 5A-5I** (C). Note that fiber implants for optogenetic experiments (A, B) were placed 0.3-0.5 mm above the VTA, while fiber photometry experiments (C) required fiber implants to be placed within the VTA.

Figure S5. Optogenetic stimulation of LH_{VGLUT2} inputs to VTA does not affect locomotor activity or anxiety but promotes aversion in a frequency dependent manner, Related to Figure 4.
(A) Schematic of real-time place preference assay, which was performed over 6 days. Each day ChR2-expressing LH_{VGLUT2} inputs to VTA were stimulated using a different frequency.
(B-G) There was no effect on place preference behavior for 1 Hz optogenetic stimulation (B; stim: 286.4 ± 48.92 s; non-stim.: 214.4 ± 36.43 s, n = 8 mice; $p = 0.416$, paired Student's t-test), whereas increasing stimulation frequencies to 2 Hz (C; stim: 134.6 ± 17.19 s; non-stim.: 382.5 ± 31.51 s, n = 8 mice; ** $p < 0.01$, paired Student's t-test), 4 Hz (D; stim: 100.1 ± 21.22 s; non-stim.: 398.8 ± 35.76 s, n = 8 mice; *** $p < 0.001$, paired Student's t-test), 10 Hz (E; stim: 68.74 ± 12.24 s; non-stim.: 465.1 ± 22.53 s, n = 8 mice; *** $p < 0.001$, paired Student's t-test) and 20 Hz (F; stim: 26.13 ± 4.69 s; non-stim.: 512.4 ± 13.45 s, n = 8 mice; *** $p < 0.001$, paired Student's t-test) caused an increase place avoidance behavior. Note that the increase in place avoidance behavior was not due to conditioning, as repeating 1 Hz stimulation (G; stim: 240.6 ± 36.44 s; non-stim.: 282.7 ± 35.16 s, n = 8 mice; $p = 0.571$, paired Student's t-test) on day 6 did not promote place aversion (data represent means ± SEM).
(H) Schematic of open field test for assessing general locomotor activity and anxiety behavior, which involves 4 Hz light stimulation of ChR2- or eYFP expressing LH_{VGLUT2} terminals in the VTA for 15 min.
(I) Representative trajectories of animals expressing ChR2 (top) or eYFP (bottom) in LH_{VGLUT2} terminals. (J) Bar graph showing no significant difference in total distance traveled (a measure of

locomotor activity) between ChR2 and eYFP groups (ChR2: 3232 ± 500.5 cm, n = 9 mice; eYFP: 3078 ± 490.5 cm, n = 10 mice; p = 0.83, unpaired Student's t-test; data represent means ± SEM).
(K) Bar graph showing no significant difference in time spent in center area (a measure of anxiety-related behavior) between ChR2 and eYFP groups (Center: ChR2: 88.76 ± 20.79 s, n = 9 mice; eYFP: 77.41 ± 19.60 cm, n = 10 mice; Corners: ChR2: 506.43 ± 50.45 s n = 9 mice; eYFP: 577.69 ± 51.84 cm, n = 10 mice; $p_{interaction}$ = 0.418, F(1,17) = 0.689, two-way RM ANOVA; Data represent means ± SEM).

Figure S6. LH neurons projecting to VTA and LHb represent largely independent projections, Related to Figure 4.
(A) Schematic showing dual injection of fluorescent retrobeads with distinct fluorophores into VTA and lateral habenula (LHb) of the same animal.
(B) Confocal images showing retrogradely labeled LH neurons projecting to LHb (green beads) and LH neurons projecting to VTA (red beads) using a 10x (upper row; scale bar: 100 μm) and 40x objective (lower row; scale bar: 20 μm).
(C) Bar graph showing that most LH neurons contain either red beads (i.e., cells that project to VTA, red bar, 62%, n = 84/135 cells) or green beads (i.e., cells that project to LHb, green bar, n = 48/135 cells). Only 2% of LH neurons are double labeled (i.e., cells that contain both red and green beads, yellow bar, n = 3/135 cells; n = 3 mice). Inset shows an example of a double-labeled LH neuron (scale bar: 20 μm).
(D-F) Same experimental design as in (A-C) but for retrobead injections into the VTA and periaqueductal gray (PAG). The bar graph shows that most LH neurons contain either red beads (i.e., cells that project to VTA, red bar, 51%, n = 152/296 cells) or green beads (i.e., cells that project to PAG, green bar, 48%, n = 141/296 cells). Only 1% of LH neurons are double labeled (i.e., cells that contain both red and green beads, yellow bar, n = 3/296 cells; n = 3 mice).

Figure S7. Selective fos immunoreactivity in LH_{VGLUT2} neurons projecting to VTA in response to an aversive stimulus, Related to Figure 5.
(A) Schematic showing injection of green retrobeads into the VTA of VGLUT2-Cre::tdTomato mice (upper panel), experimental timeline (middle panel) and coronal section showing retrobead (green) injection site in the VTA (lower panel; scale bar: 100 μm).
(B, C) Confocal image showing retrogradely labeled (green, beads) glutamatergic (tdT-positive, red) LH neurons that project to the VTA (arrows). Animals that have been exposed to formaldehyde (B) display increased fos (white) immunoreactivity in these neurons compared to control (ctrl) mice, which interacted with a novel object (C; Scale bars: 10 μm).
(D) Bar graph showing a significant increase in total number of fos-immunopositive cells in the LH of animals exposed to formaldehyde (form) compared to ctrl animals (form: 333.8 ± 17.68 cells, n = 4 mice; ctrl: 149.3 ± 17.92 cells, n = 4 mice; *** p < 0.001, unpaired Student's t-test; data represent means ± SEM).
(E) Bar graph showing no significant difference in the mean number of retrogradely labeled tdT-positive LH neurons between animals exposed to form and ctrl animals (form: 47.46 ± 4.31%, n = 4 mice; ctrl: 44.18 ± 4.51%, n = 4 mice; p = 0.618, unpaired Student's t-test; data represent means ± SEM).
(F) Bar graph showing significant increase in fos-immunoreactivity in retrogradely labeled, tdT-positive LH neurons projecting to VTA in response to form exposure compared with ctrl

animals. Form exposure does not alter fos-immunoreactivity in retrogradely labeled, tdT-negative (i.e., putative GABA neurons) LH neurons projecting to VTA (form: tdT-pos. 18.76 ± 2.21%, tdT-neg. 7.70 ± 1.34%, n = 4 mice; ctrl: tdT-pos. 10.06 ± 1.39%, tdT-neg. 7.56 ± 0.97%, n = 4 mice; ** $p < 0.01$; two-way ANOVA with Holm-Sidak's post-hoc test; data represent means ± SEM).

Figure S8. Ablation of LH_{VGLUT2} neurons and fiber photometry in the vNAcMed, Related to Figure 8.
Bar graphs showing terminal activity (quantified as area under the curve, AUC) in the vNAcMed before (first shock trial, red) and after aversive conditioning (last shock trial, blue) for mice expressing mCherry (left bar graph; tone: first: 2.18 ± 1.41; last: 36.47 ± 4.45; shock: first: 63.1 ± 5.37; last: 44.73 ± 7.85, n = 4 mice, two-way RM ANOVA, p(interaction) < 0.001 with Holm-Sidak post-hoc test, p(tone) = 0.003, p(shock) = 0.022) or Caspase 3 (CASP, right bar graph; tone: first: 2.19 ± 2.44; last: -4.01 ± 4.5; shock: first: 65.28 ± 5.18; last: 26.19 ± 9.97, n = 4 mice, two-way RM ANOVA, p(interaction) = 0.038 with Holm-Sidak post-hoc p(tone) = 0.506, p(shock) = 0.009) in LH_{VGLUT2} neurons (data represent means ± SEM). Note that the reduction in response to foot shock after aversive conditioning in Figure 1H is slightly more pronounced, which could reflect the differences between recordings in head-fixed versus freely-moving animals. Although the foot shock had the same intensity (0.4 mA) and duration (2 sec), it may be more aversive when administered in a head-fixed setup, since it is unescapable (i.e., by jumping, as shown see Supplementary Video 1).

Supplementary Tables

Supplementary Table 1. Quantification of monosynaptic rabies virus tracing, Related to Figures 3 and 6.
(A) Quantification of presynaptic input in different brain structures to vNAcMed-projecting DA neurons or NAcLat-projecting DA neurons.
(B) Quantification of *in situ* hybridization (ISH) experiments for cells in the LH, which express VGLUT2 and synapse onto different VTA cell populations.

Supplementary Movies

Supplementary Movie 1. Simultaneous *in vivo* fiber photometry recordings of dopamine terminals in the ventral NAcMed and NAcLat during the tone-shock conditioning paradigm (Related to Figure 1; Note that the orange line indicates duration of tone, while the blue line refers to the foot shock).

Supplementary Movie 2. Representative example (2x speed) showing optogenetic stimulation of LH_{VGLUT2} terminals in the VTA during the real-time place aversion assay (Related to Figures 4A-4F).

Supplementary Movie 3. Representative example showing optogenetic inhibition of LH_{VGLUT2} terminals in the VTA during the formaldehyde approach/avoidance assay (Related to Figures 4G-4M; left: control; right: NpHR).

Supplementary Movie 4. *In vivo* fiber photometry recordings of LH_{VGLUT2} terminals in the VTA during the formaldehyde approach/avoidance assay (Related to Figures 5A-5I; 5x speed, note that the speed of the video is intentionally decreased to 0.5x when the mouse approaches the formaldehyde stimulus).

Figure S1 de Jong, Afjei et al.

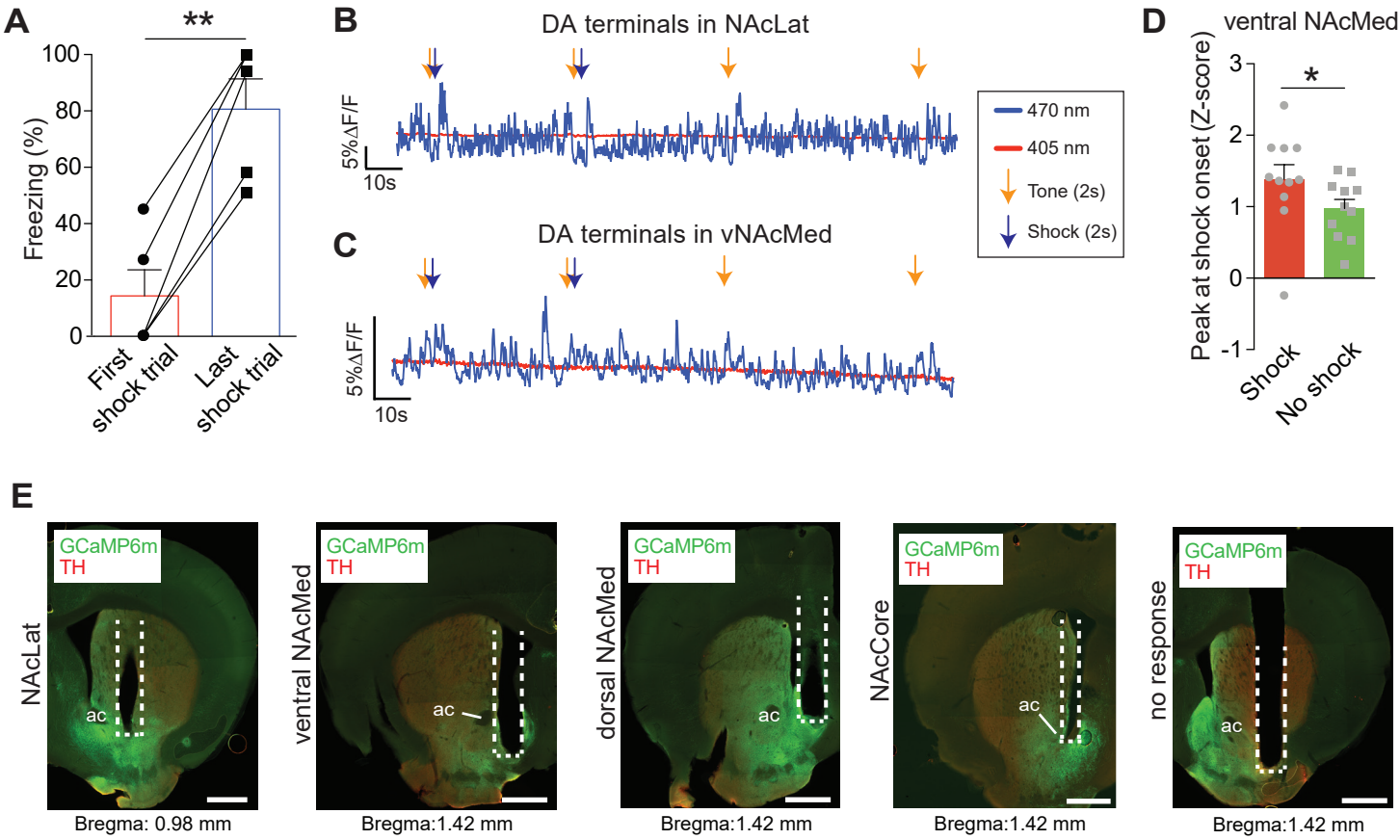

Figure S2 de Jong, Afjei et al.

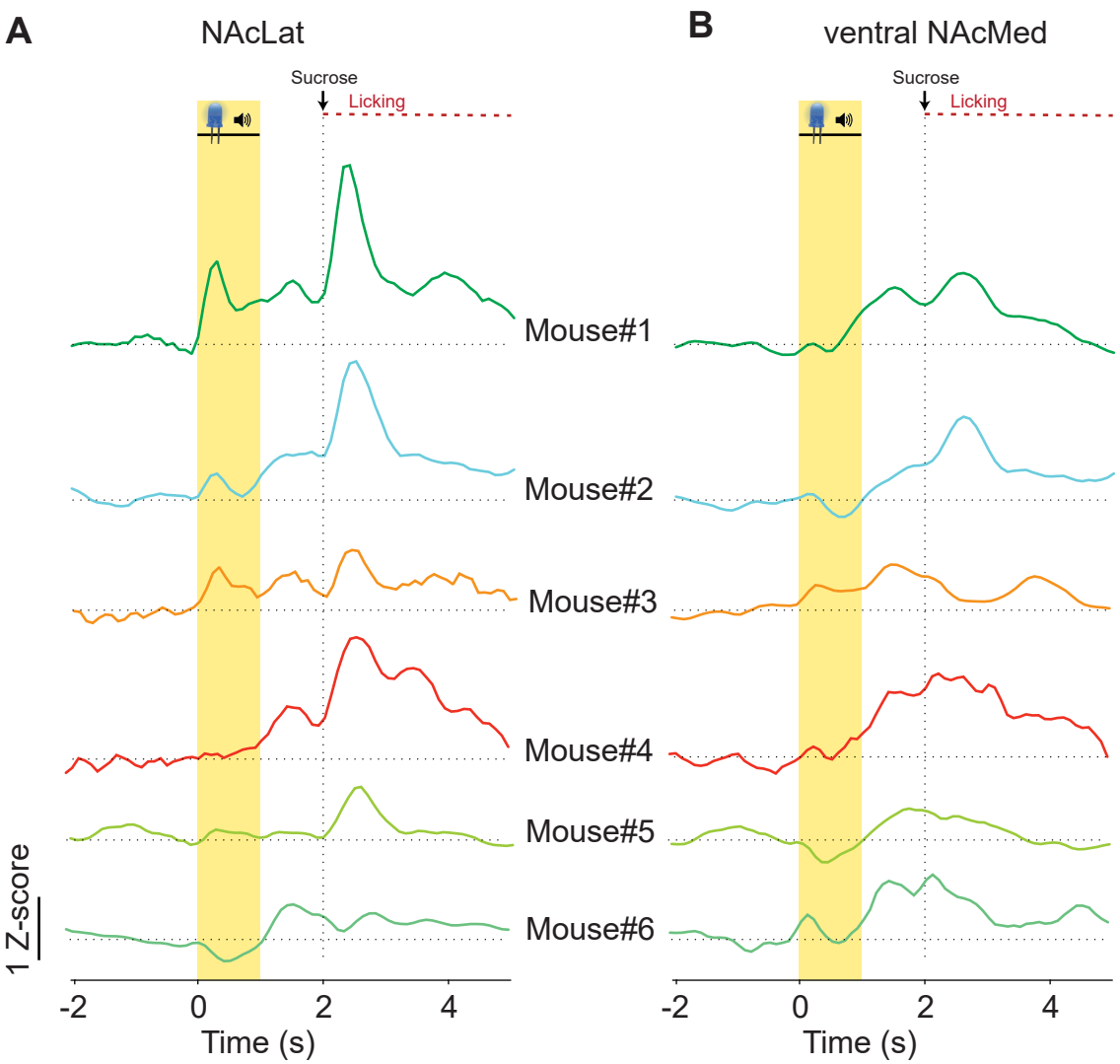

Figure S3 de Jong, Afjei et al.

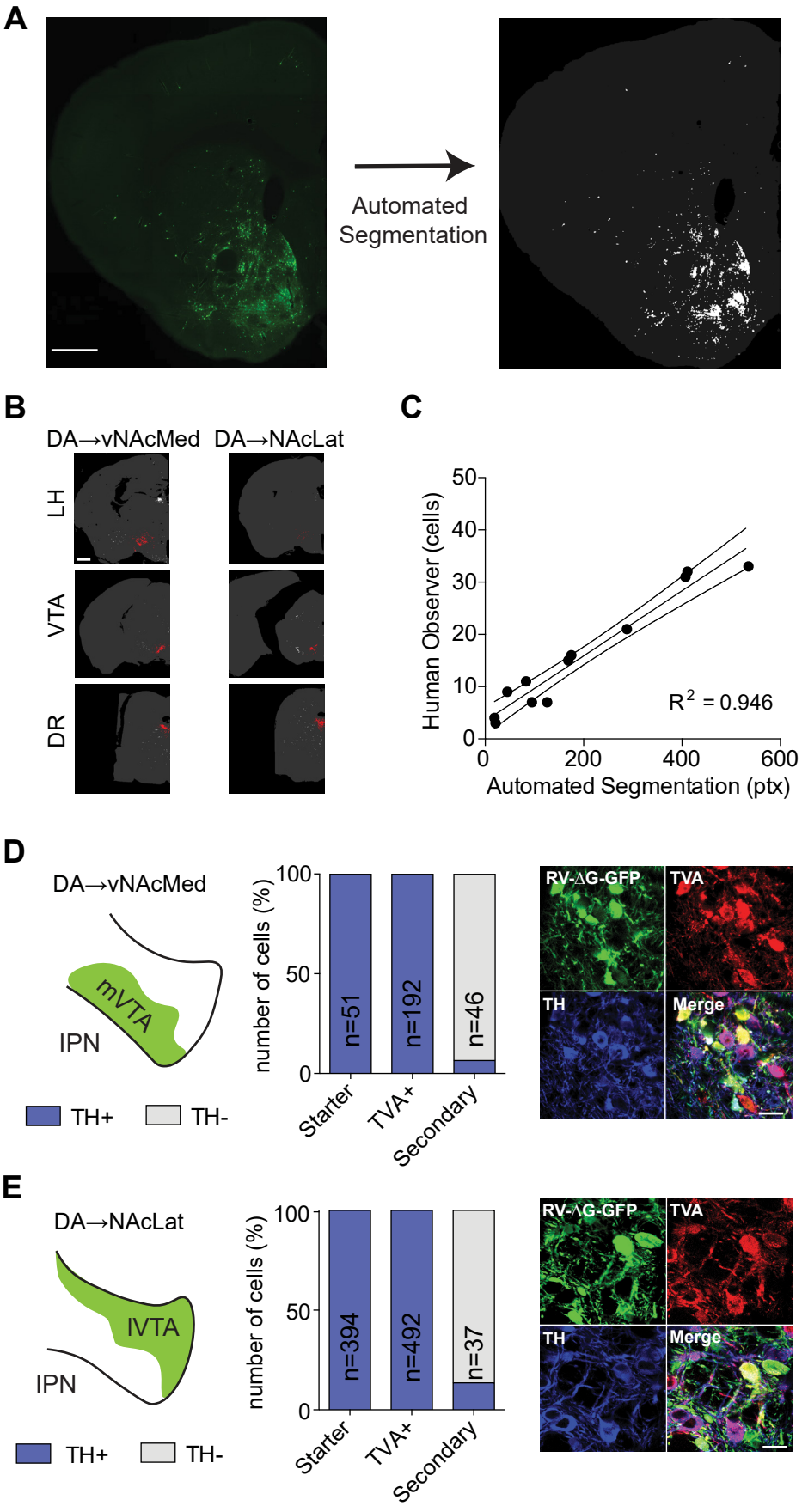

Figure S4 de Jong, Afjei et al.

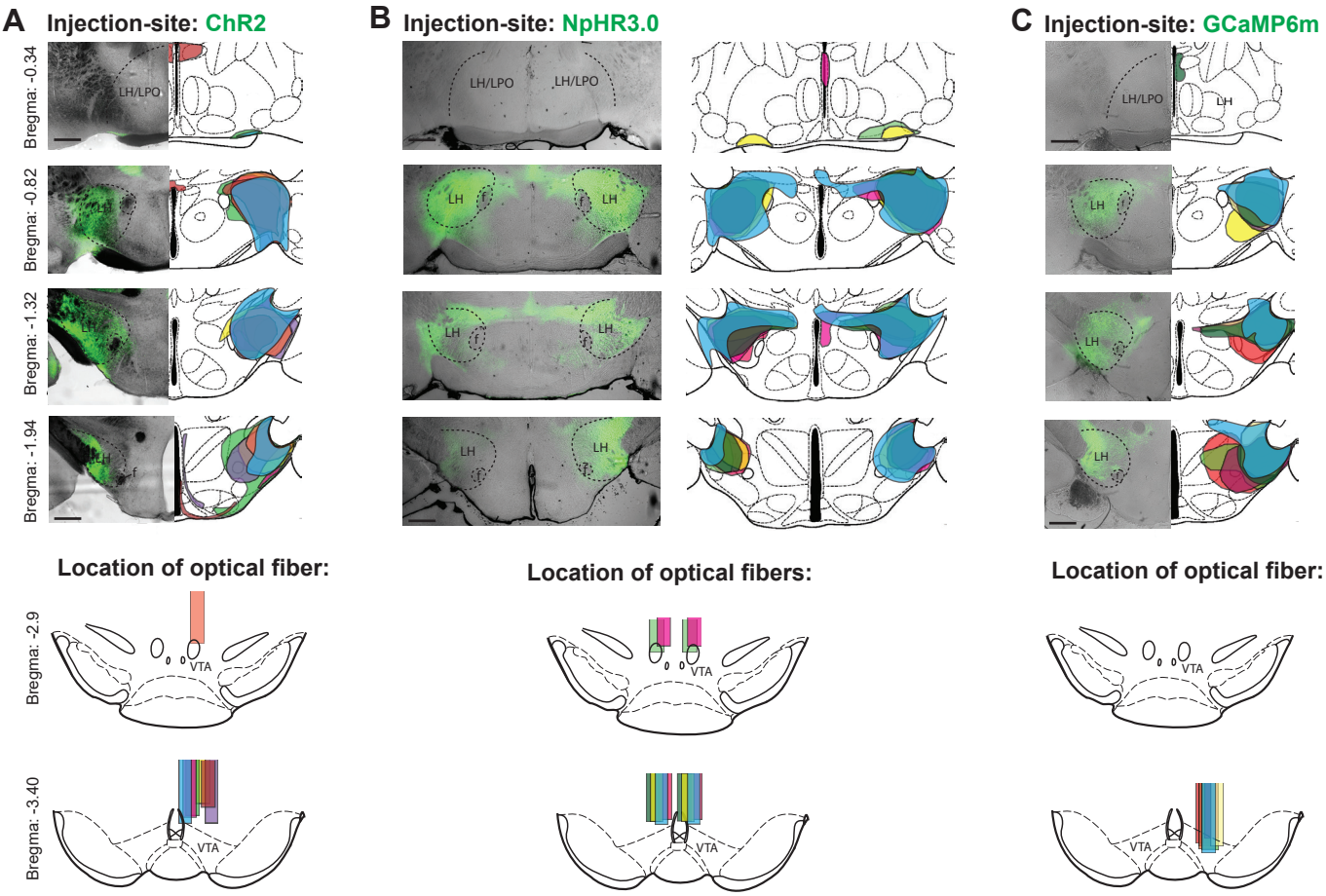

Figure S5 de Jong, Afjei et al.

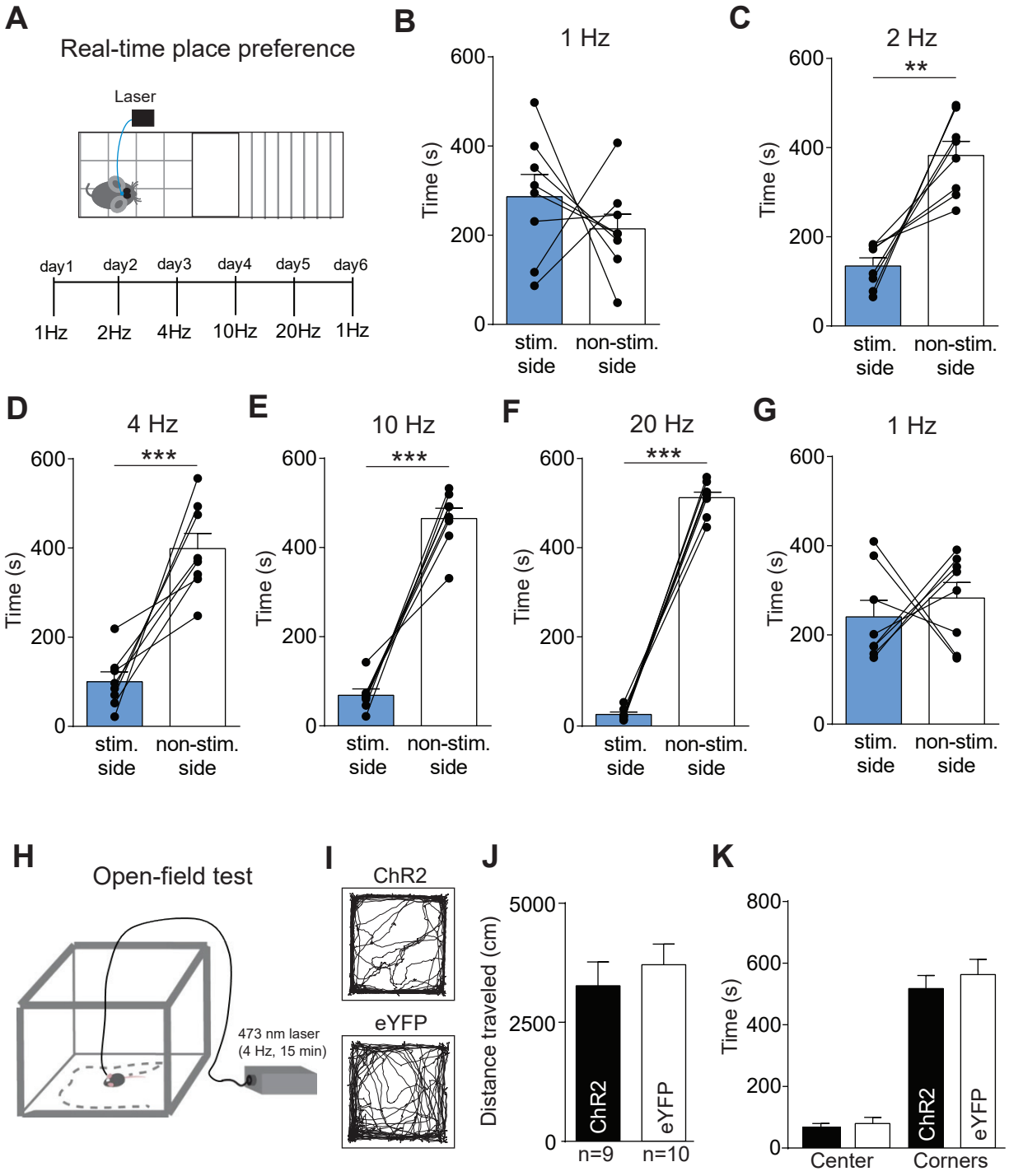

Figure S6 de Jong, Afjei et al.

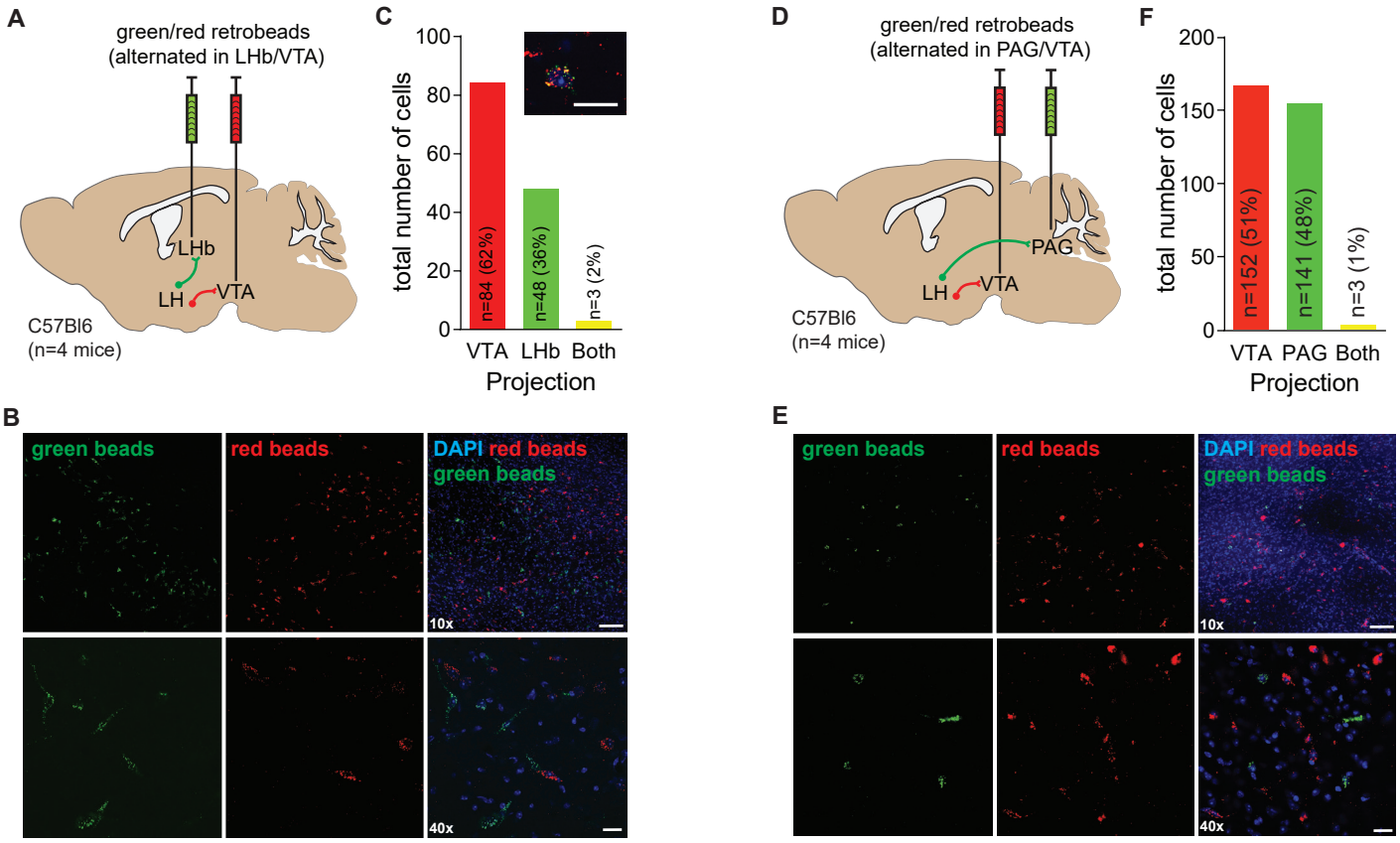

Figure S7 de Jong, Afjei et al.

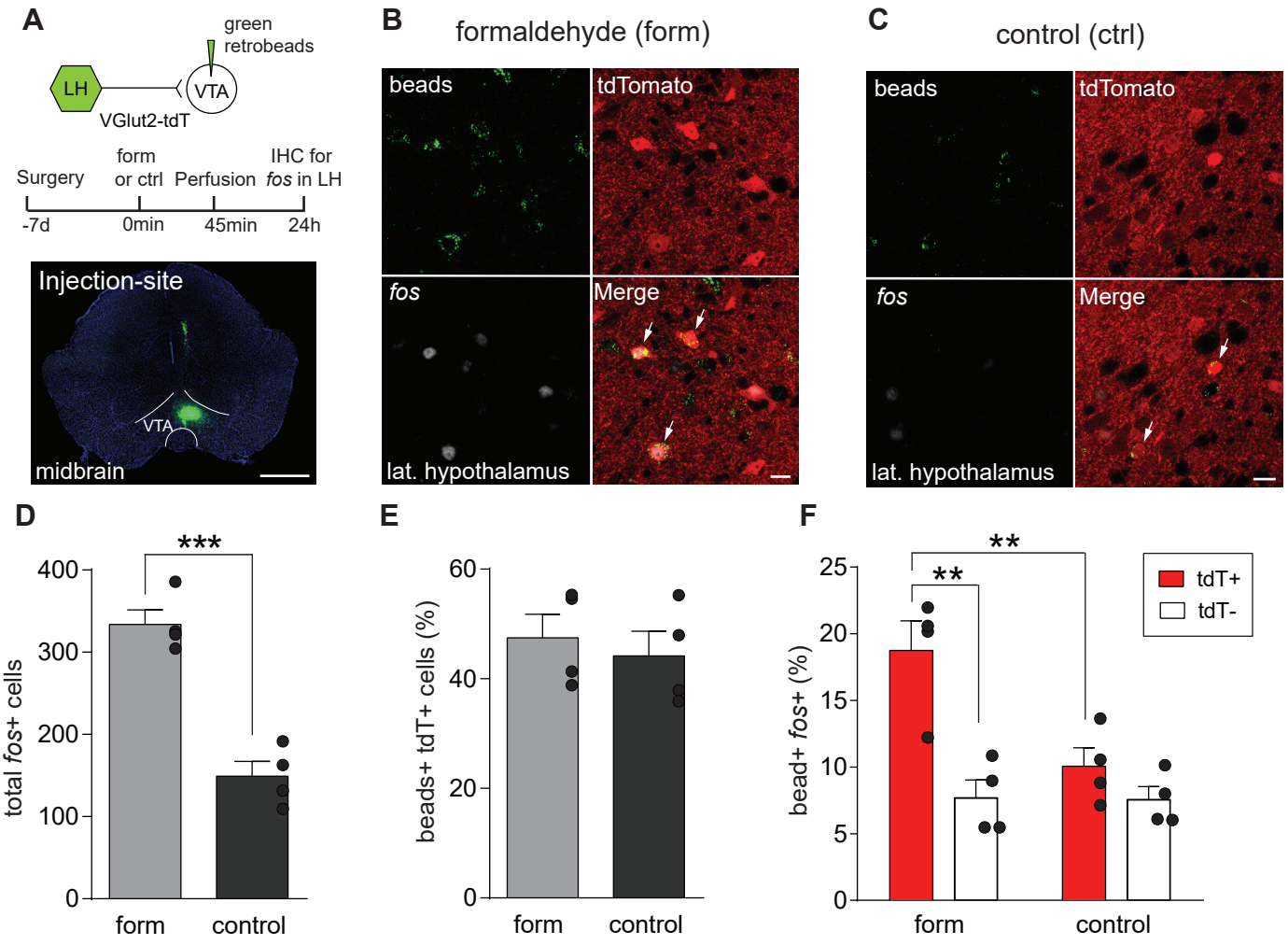

Figure S8 de Jong, Afjei et al.

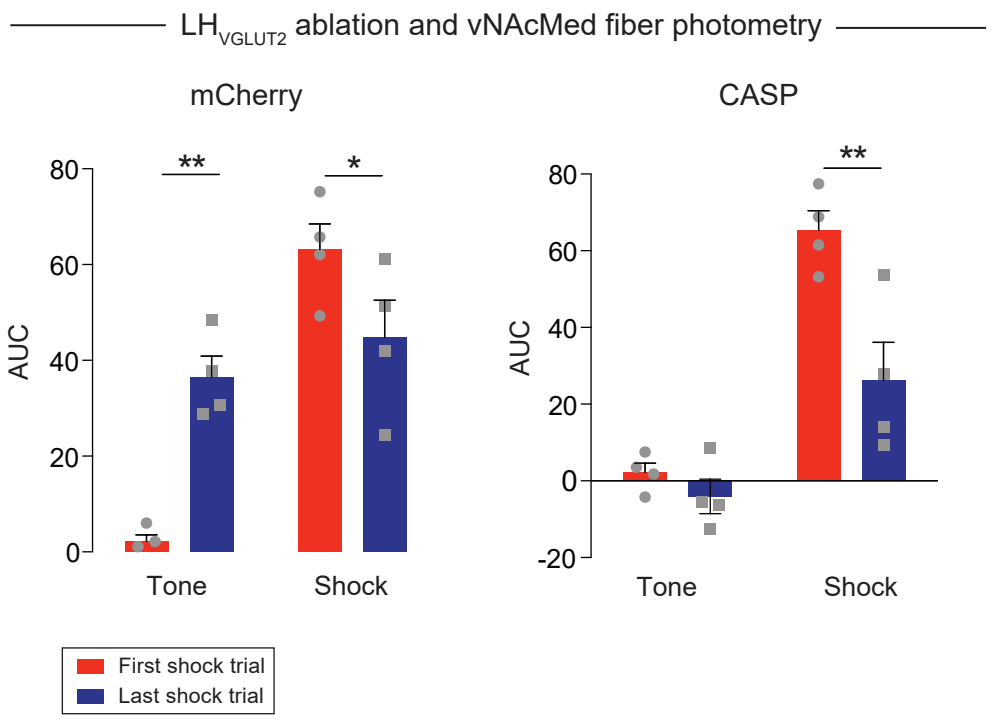

Supplementary Table 1 de Jong, Afjei et al.

A

	N	Total	VTA	Presynaptic Input (px) OFC	mPFC	DMS	DLS	NAcCore	NAcMed	NAcLat	VP	BNST	GP
VTA_{DA}→vNAcMed	4	136764 ± 65337	36143 ± 14256	619 ±519	992 ±654	220 ±134	3 ±2	2883 ±2576	9113 ±5702	630 ±410	10857 ±7864	2607 ±2155	480 ±381
VTA_{DA}→NAcLat	5	92106 ±63107	31861 ±18762	258 ±205	238 ±183	1157 ±918	22 ±15	2078 ±1529	4216 ±3456	1479 ±1229	5454 ±3602	2196 ±1853	1197 ±958

Presynaptic Input (px) PO	LH	PVN	CeA	LHb	MHb	STh	DR	LDT	LPB
1896 ±1483	17112 ±9392	1308 ±842	1052 ±843	2897 ±1525	447 ±267	373 ±233	42801 ±21728	3648 ±1854	686 ±424
303 ±180	10519 ±8132	596 ±414	1242 ±1083	319 ±170	65 ±44	515 ±275	26603 ±19232	1228 ± 788	559 ±541

B

Projection:	N	Avg. Labeled Cells	ISH+
VTA_{DA}→vNAcMed	3	259 ±32.1	88 ±9.0
VTA_{DA}→NAcLat	3	94 ±5.8	24 ±1.2
VTA_{GLUT}→vNAcMed	3	160 ±27.5	43.3 ±11.9
VTA_{GABA}	2	12.5 ±5	3.5 ±2